Dielectric properties of confined ionic liquids

Pat Sippel, Stephan Krohns, Dmytro Denysenko, Dirk Volkmer

Angaben zur Veröffentlichung / Publication details:

Sippel, Pat, Stephan Krohns, Dmytro Denysenko, and Dirk Volkmer. 2018. "Dielectric properties of confined ionic liquids." In Proceedings of the 12th Pacific Rim Conference on Ceramic and Glass Technology: a cllection of papers presented at the 12th Pacific Rim Conference on Ceramic and Glass Technology, May 21-26, 2017, Waikoloa, Hawaii, edited by Dileep Singh, Manabu Fukushima, Young-Wook Kim, Kiyoshi Shimamura, Nobuhito Imanaka, Tatsuki Ohji, Jake Amoroso, and Michael Lanagan, 191–99. Westerville, OH: The American Ceramic Society. https://doi.org/10.1002/9781119494096.ch19.

DIELECTRIC PROPERTIES OF CONFINED IONIC LIQUIDS

Pit Sippel, Stephan Krohns
Experimental Physics V, University of Augsburg
86159 Augsburg, Germany

Dmytro Denysenko, Dirk Volkmer
Solid State Chemistry, University of Augsburg
86159 Augsburg, Germany

ABSTRACT

Ionic liquids, as solvent free electrolytes, are promising materials improving the energy density of future storage devices. Two key requirements for such an application are a broad electrochemical window and a high ionic mobility of ionic liquids. A thorough measurement of the dielectric properties in a broad temperature and frequency regime allows analyzing the latter one in detail. Ionic mobility is influenced by intrinsic relaxations. These relaxations are influenced by correlation between the molecules. Confining the molecules allows to access this correlation length and to address the fundamental questions regarding supercooled liquids. We demonstrate this by confining the ionic liquid 1-butyl-3-methyl-imidazolium chloride in a metal-organic-framework, namely MFU-4. The preliminary results of an enhanced rotational motion compared to the bulk ionic liquid point towards a temperature, where the correlation length corresponds to the pore diameter of the confining host.

INTRODUCTION

Ionic liquids are salts that are molten below about 373 K. They are often ascribed as designer solvents due to the large number of possible cation and anion compositions in combination with their chemical tunability [1]. A huge amount of publications on these materials [2,3] demonstrates their importance and versatility for future applications. Since they are basically solvent free electrolytes, i.e., solely ions in the liquid state, they are promising for the application in energy storage devices [4,5,6,7]. Other advantages of ionic liquids are their low volatility and high electrochemical stability. However, the conductivity of the known ionic liquids cannot compete with that of conventional electrolytes. A fundamental understanding of their dynamical properties can pave the way to find and optimize an ionic liquid with the required ionic mobility and thus an enhanced conductivity.

Most ionic liquids are glass-forming liquids. The glass transition and glassy dynamics play an important role in these systems [8]. The investigation of liquids confined in host materials has proven to be a very useful tool gaining information about the glass transition in general [9,10,11,12,13,14]. Ionic liquids are one of the most prominent topics in materials research leading to interesting theoretical and experimental studies of these ionic liquids in confinement as shown, e.g. in refs. [15,16,17,18,19,20,21]. Various materials are available as host lattice for confinement studies [13]. In the present work, we use a metal-organic framework (MOF), namely MFU-4 [22]. MOFs in general are composed of metal ions or clusters that are linked by organic ligands into three-dimensional crystalline framework structures exhibiting the required porosity [23,24,25,26,27,28]. Due to their low dielectric constant and leakage currents they are suited as new interlayer dielectric materials to improve integrated circuits [29]. The same properties make them useful as host materials for confinement measurements. Particularly, the size and high regularity of their pores are outstanding compared to conventional porous materials for confinement measurements [14]. We succeeded to confine the ionic liquid 1-butyl-3-methyl-imidazolium chloride (BMIM-Cl) in the host MFU-4 by employing the ionic liquid as

a co-solvent in the synthesis. The dynamic processes and conductivity of this sample are analyzed via dielectric spectroscopy.

EXPERIMENTAL

To prepare BMIM-Cl confined in MFU-4 (BMIM-Cl@MFU-4) H_2-BBTA ligand (280 mg, 1.75 mmol) and lithium hydroxide monohydrate (147 mg, 3.5 mmol) were dissolved under reflux in absolute ethanol (12 mL). After cooling down to room temperature, a solution of anhydrous zinc chloride (955 mg, 7 mmol) and BMIM-Cl (7 g, 40.1 mmol) in absolute ethanol (8 mL) was added under stirring. White precipitate appeared immediately after addition. The mixture was heated at 90 °C under reflux for 16 h. After cooling down to room temperature, the precipitate was filtered off and washed with absolute ethanol (4x10 mL) and dichloromethane (3x10 mL). The product was dried in vacuum at 150 °C for 2 h. The yield was 960 mg.

The purity of the product was proven by XRPD analysis (Seifert XRD 3003 TT diffractometer) and IR spectroscopy (Bruker Equinox 55 FT-IR spectrometer). IR spectra of products show bands characteristic for both, MFU-4 and BMIM-Cl. XRPD patterns show reflexes, characteristic for MFU-4 framework and thus confirm the phase purity. However, the reflexes are considerably broader, as compared to MFU-4, pointing at lower crystallinity of BMIM-Cl@MFU-4. TGA-measurements (TA Q500) show, that the solvent (ethanol) can be removed at 150-200 °C. Heating the sample at 200 °C for 16 h in vacuum resulted in partial removal of BMIM-Cl from the pores, producing the sample with low content of IL. Heating for 2 h at 150 °C in vacuum allows to remove ethanol as well while BMIM-Cl remains in the pores, giving the sample with high content of IL. The content of IL was determined by ^{1}H NMR spectroscopy (Varian mercury plus 400) after dissolving dried sample (30 mg) in a mixture of DMSO-d_6 (0.5 mL) and DCl (20 % in D_2O, 0.1 mL). The molar ratio BMIM-Cl/H_2-BBTA in solution (1:1 for sample 1 and 0.13:1 for sample 2) corresponds to approx. 6 molecules per pore (sample 1) and 0.8 molecules per pore (sample 2).

The complex permittivity and the real part of the conductivity covering a frequency range of about 10 mHz – 67.2 kHz were measured using a frequency-response analyzer (Novocontrol α-analyzer). For sample cooling and heating between 130 and 330 K, a closed-cycle refrigerator was equipped. All dielectric measurements were performed in vacuum to exclude effects based on residual water. The powder samples were used as dielectric material in a parallel-plate capacitor, with sample thicknesses of 150 (sample 1) and 230 µm (sample 2). For sample 1a and 2 the top electrode compressed the powder while measuring the dielectric properties. For sample 1b no pressure was applied via the top electrode. In addition to the pressure-induced impact on the dielectric properties, also the limited packing density of the powder may reduce the obtained absolute values of the measured dielectric permittivity. To remove residual water absorbed from air during sample preparation the prepared capacitors were mounted into the sample chamber and kept in vacuum (at least for 48 hours) prior to the consecutive measurements.

RESULTS AND DISCUSSION

Figure 1 shows the dielectric constant (a) of sample 1a and 1b (these samples differ in the pressure on the dielectric material induced from the top electrode; see experimental) for various frequencies recorded while cooling the sample. These samples have an amount of ionic liquid with approximately 6 BMIM-Cl molecules inside the pores of the metal-organic framework. At low temperatures the dielectric permittivity of sample 1a approaches an almost frequency-independent value of about 1.5. This frequency-independent limit for high frequencies and low temperatures is regarded as ε_∞ and represents the ionic and electronic polarizability. The metal-organic frameworks are known for their very low dielectric constants

[29]. Since empty MFU-4 has a $\varepsilon_\infty \approx 1.8$ [30] and the bulk ionic liquid reveals $\varepsilon_\infty \approx 3$ [31], the overall value should be higher than 1.5. However, due to the powder form of the samples the observed values are most likely affected by its packing density, dependent on the size of the powder grains. At temperatures above 230 K the real part of permittivity increases via a

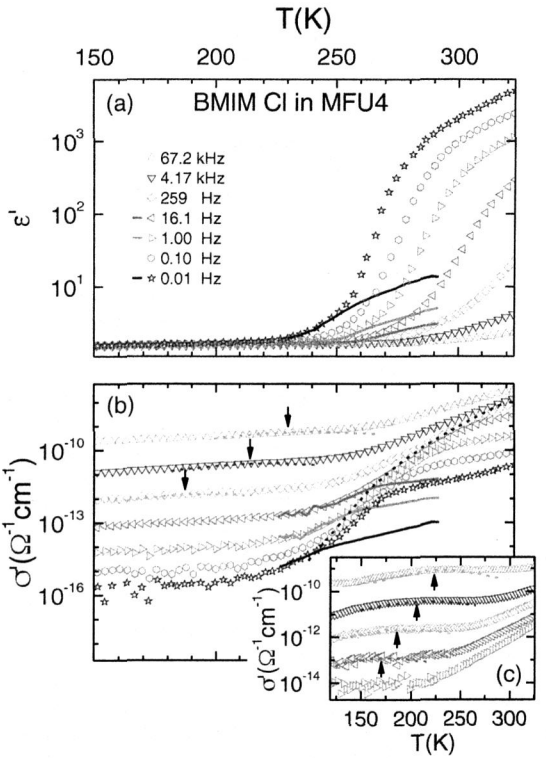

Figure 1. Temperature dependence of the dielectric constant (a) and conductivity (b) of BMIM-Cl confined in MFU-4 (sample 1a) for various frequencies. The lines represent three frequencies of sample 1b, where the spectra have been recorded with reduced pressure. The inset (c) is the temperature dependence of the conductivity of sample 2 that has a lower loading fraction. The dashed lines with the arrows illustrate the intrinsic relaxation and the black dashed line indicates the dc conductivity.

significant step. This step is a typical signature for a relaxation, i.e., ε' shifts to higher temperatures for increasing frequencies. But, the colossal dielectric constants, i.e., $\varepsilon' > 1000$ [32] at temperatures above 280 K for frequencies $\upsilon < 1$ Hz, clearly indicate an extrinsic origin. Internal insulating interfaces or blocking electrode layers at the electrodes often create a very high apparent dielectric constant, because they can act as thin insulating layers within the bulk material leading to a high capacitance [33]. This contribution to the spectra is called Maxwell-Wagner-relaxation mimicking an intrinsic relaxation. To clarify the extrinsic nature of this dielectric feature we performed a measurement on sample 1b, where we modified sample-

electrode contact area using a reduced pressure of the top electrode. The lines represent the results of sample 1b in Figure 1 for 16.1 Hz, 1 Hz and 10 mHz. An intrinsic feature should be independent of this pressure, against the capacitances of surface layers are influenced by the area of electrode-sample contacts and the thickness of a barrier layer formed at these interfaces. In the present case, a lower pressure on the top electrode decreases the surface area between the powder grains and electrodes due to lower surface packing density. Such a decreased surface area leads to a lower dielectric constant of an accompanied Maxwell-Wagner relaxation. Indeed the sample 1b (lower pressure) reveals a decrease by two orders of magnitude of the colossal dielectric constant plateau, e.g., 10 mHz around 290 K. For T < 250 K the dielectric spectra of both samples merge evidencing the real intrinsic properties.

Figure 1b shows the temperature-dependent conductivity of sample 1a. For T < 250 K an almost temperature independent conductivity is revealed for various frequencies. These plateau-like features are shifting to higher values for higher frequencies. Such a frequency-dependence could arise from the so-called universal dielectric response [34], a power law $\sigma'(\upsilon) \propto \nu^s$ with $s < 1$. However, a broadened relaxation would create the same characteristic feature. A separation between these effects can be done by a thorough equivalent circuit analysis, which is not in the focus of this study. A rather small change of slope in these plateaus shows the presence of a relaxation creating a frequency-dependent local maximum, which is denoted by the dashed lines, e.g., around 210 K for the 4.17 kHz curve. The black arrows indicate the estimated maxima, which can be used to reveal the characteristic relaxation time via $2\pi\nu(T) = 1/\tau(T)$. At temperatures above 250 K the conductivity increases and the different frequencies merge leading to almost the same temperature dependence, e.g., around 270 K for the 0.1 Hz- and the 1 Hz-curve. This behavior normally indicates the temperature dependent dc-conductivity (dashed line). The transition between the low-temperature plateaus and the assumed dc-conductivity is rather shallow pointing towards one or several superimposed relaxations. Unfortunately, there is no characteristic change in slope and we can only speculate about its presence. For measurements, which are on the right side of the dc-conductivity, the properties of sample 1b and 1a strongly differ, due to the above mentioned surface layer effect. In this region the conductivities of the lower frequencies are decreasing. Again, this is caused by the interfaces in the sample (compare lines and symbols) and is not discussed in detail.

The inset (Figure 1c) shows the temperature dependence of the conductivity of sample 2, which has an average filling of one MFU-4 pore with about 0.8 molecule of BMIM-Cl. For comparability the same symbols represent the same frequencies as for sample 1a. At temperatures below 225 K the conductivity is almost temperature independent and again shifts to higher values for higher frequencies. Surprisingly, the intrinsic relaxation shows up as distinct features and the arrows indicate their estimated peak positions. The dashed lines emphasize the local maxima in the curves. Interestingly, this relaxation of sample 2 is stronger (the local maxima are higher) than the relaxation of sample 1, despite the lower amount of BMIM-Cl. Probably, the rotation of the cations is hampered in sample 1, due to the more packed filling. This results in a lower overall polarization and a smaller contribution to the feature observed in the conductivity spectra. At higher temperatures there is a steady increase, starting at lower frequencies. In contrast to the previous sample 1a there is no clear frequency independent regime. The dc-conductivity of sample 2 is lower than for sample 1a and probably too low to show a clear signature in the given frequency and temperature window. Only the frequencies 16.1 Hz and 1 Hz indicate their merging for temperatures above 315 K. We use the measurement points of the 1 Hz curve above 315 K as an estimate for the dc-conductivity in the following discussion. The reduced conductivity of this sample can be explained by the reduced amount of ionic liquid. Since the pure metal-organic-framework has a low conductivity [30], mainly the ions of the ionic liquid contribute to the dc-conductivity of the sample. In the case of

sample 2 the amount of charge carriers is reduced leading to the observed decreased conductivity. However, the underlying conduction mechanism has to be investigated clarifying, e.g., if the chloride ions are responsible for hopping conductivity.

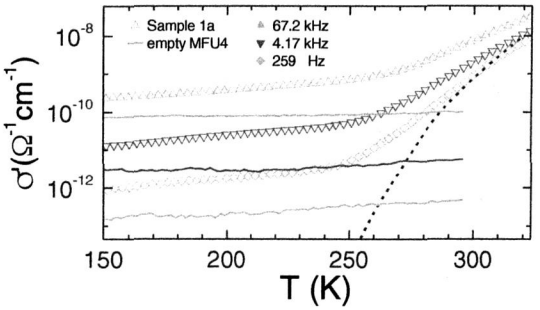

Figure 2. Comparison of the temperature dependence of the conductivity of sample 1a and empty MFU-4 at selected frequencies. The dashed line indicates the dc-conductivity.

Figure 2 shows the conductivities of sample 1a compared to pure MFU-4 for selected frequencies. Pure MFU-4 (lines in Fig. 2) has an almost temperature independent conductivity without any signatures of relaxations in the selected temperature range. In comparison to sample 1a the conductivity is more than one order in magnitude lower and no indication of the temperature dependent dc-conductivity is revealed. The confinement of BMIM-Cl in MFU-4 clearly increases the conductivity and the samples also exhibit the discussed intrinsic relaxation. This proves, that the relaxation is based on dipolar contributions of the ionic liquid rather than a dielectric feature of the MFU-4.

Figure 3 illustrates the relaxation times τ and the dc-conductivities of samples 1a and 2 in comparison to pure BMIM-Cl in an Arrhenius representation. Pure BMIM-Cl exhibits an intrinsic relaxation based on the reorientation of the dipolar cation [31]. Generally, this main relaxation follows a non-Arrhenius temperature dependency, which is observed for the structural relaxation in many supercooled liquids. The Vogel-Fulcher-Tammann (VFT)-equation is commonly used to parameterize this temperature dependency of the structural relaxation of glassy matter [35]. The dashed line in Figure 3 represents that VFT-fit. Since the dc-conductivity, which is in ionic liquids often the pure translational motion of ions, is related to the viscosity of ionic liquids, σ_{dc} also follows a non-Arrhenius temperature dependency. Interestingly, for BMIM-Cl the temperature dependent dc-conductivity as well as the main relaxation can be scaled onto each other, as shown in Figure 3 (closed and open symbols). Furthermore, pure BMIM-Cl exhibits a secondary intrinsic relaxation showing up at lower temperatures and shorter relaxation times (closed triangular symbols) [31].

The confined samples 1a and 2 differ significantly from the spectra of pure BMIM-Cl. Both, the relaxation time and the possible dc-conductivity follow an Arrhenius-law that is indicated by the straight lines in Figure 3. The dc-conductivity of sample 1a is decreased by about 5 orders in magnitude compared to BMIM-Cl, e.g., at 320 K (= 3.1 [1000/K]), for sample 2 more than 8 orders, respectively.

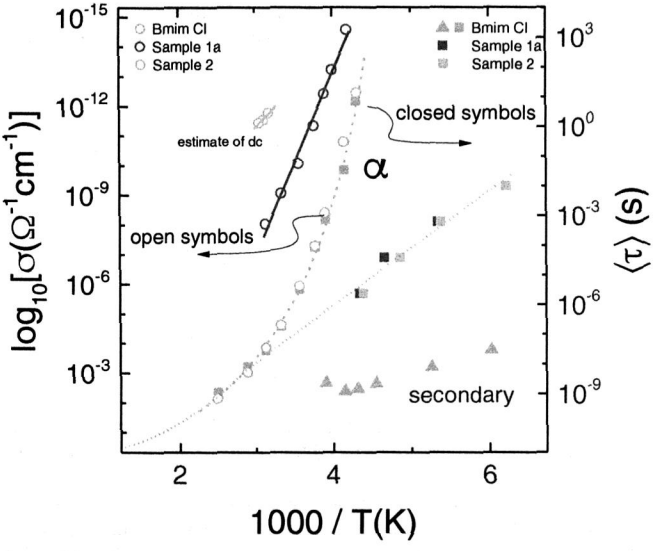

Figure 3. Relaxation times (closed symbols) and dc-conductivities (open symbols) in an Arrhenius representation of bulk BMIM CL and BMIM Cl confined in MFU-4. The data are revealed from the dielectric properties of sample 1a and sample 2. The properties of bulk BMIM-Cl were taken from Ref. 31. The dashed line represents a fit with the Vogel-Fulcher-Tammann-equation. The dotted line serves as a guide to the eye for the confinement effect. The straight lines through the circles indicate the linearity of the conductivity in this representation.

In contrast, the dielectric relaxation in both samples has the same relaxation time. The closed square symbols can be described by the dotted line. This finding indicates a common origin of this relaxation, which is most likely the reorientation of the cations as it is the strongest intrinsic relaxation in the pure ionic liquid. In confinement the relaxation time seems to be dramatically reduced. A considerably modification of molecular dynamics is found for many confined glass formers and also for ionic liquids, e.g., refs. [9,10,11,12,13,15,16,20]. A possible explanation are Maxwell-Wagner effects arising from the electrical heterogeneity of the confined samples, which can influence the relaxation time of the reorientational processes shifting it towards higher frequencies [36]. However, in the present case we exclude this effect since sample 1a and sample 2 with different ionic liquid filling ratios do not exhibit a shift in the relaxation time. In many cases the shift of relaxation times is caused, e.g., by wall interaction or steric hindrance of strongly confined systems. Here, the decrease of τ implies a reduced interaction compared to the bulk ionic liquid and can be caused by the so-called confinement effect. The accompanied typical deviation from Arrhenius behavior can be interpreted in terms of an increased effective energy barrier, when the liquid is approaching the glass transition [37]. This increase is based on the growth of cooperative motion of the molecules. As the liquid is confined to several molecules this growth is limited. This should cause a transition from VFT-

to Arrhenius-behavior approaching this limit, which leads to an increase of the effective energy barrier at a certain temperature. Such a transition was only observed in some cases [10,12,13]. In that scenario the relaxation time should mimic the bulk behavior until the confinement limit is reached. The dotted line in Figure 3 indicates such a scenario. It should be noted, that the relaxation strength and the broadening of the intrinsic relaxation is slightly above the resolution-limit giving rise to possible deviations. A final proof of the scenario requires further measurements at temperatures above 360 K and frequencies above 1 MHz. The transition temperature and the cooperativity length of confined matter is a very interesting research field and the present are promising that confining ionic liquids in metal-organic frameworks can access this fundamental properties.

Furthermore, the opposite shift of molecular rotation (decreased relaxation time) and the indications for dc-conductivity (reduced compared to bulk) is substantial. The different shift and slope of the two processes in contrast to the bulk ionic liquid, signifies a possible decoupling between them. This enables to separate the Maxwell-Wagner effects from the rotational motion, to study the latter in more detail. Especially, in glass forming liquids the dynamical properties play an outstanding role for the properties of the liquid.

CONCLUSION

Confining an ionic liquid opens a route to investigate intrinsic relaxations and the impact of glass transition on the dielectric properties, which are often in bulk materials superimposed by extrinsic effects. Therefore, we prepared two concentrations of confined BMIM-Cl, about 0.8 and about 6 molecules per pore, in the pores of a metal organic framework, namely MFU-4. The ionic liquid was included within the solvent during the synthesis of the metal-organic framework. Broadband dielectric spectroscopy in a temperature range from 150 K to 330 K reveals for the confined samples a rather low conductivity compared to the pure ionic liquid, which further depends on the filling ratio of the pores with the ionic liquid. The latter effect points towards a reduced charge carrier density for the 0.8 molecule per pore sample. In addition, the dielectric spectra show the signature of relaxation, with the same relaxation time for both samples. This relaxation is most likely based on the reorientation of the cations, with a strongly decreased relaxation time compared to the bulk ionic liquid. Extrapolations of the relaxation times suggest that the confinement effect hampers the retardation of the relaxation times while cooling the sample. To clarify the impact of the confinement effect on intrinsic relaxations further measurements at higher temperatures and lower frequencies are necessary. In this work, we demonstrate that confining BMIM-Cl in MFU-4 allows analyzing intrinsic relaxations and the impact of glass transition, which is a feasible way to experimentally access the correlation length in ionic liquids.

ACKNOWLEDGEMENTS

This work was supported by the BMBF via the project ENREKON 03EK3015.

REFERENCES

[1] Weingärtner H. (2008). Understanding ionic liquids at the molecular level: facts, problems, and controversies, *Angew. Chem. Int. Ed., Vol. 47,* 654-670.

[2] Endres F. & Abedin S.Z.E. (2006). Air and water stable ionic liquids in physical chemistry, *Phys. Chem. Chem. Phys., Vol. 8,* 2101-2116.

[3] Rogers R.D., Zhang S.J. & Wang J.J. (2012). Preface: An International Look at Ionic Liquids, *Sci. China Chem., Vol. 55,* 1475-1477.

[4] Armand M., Endres F., MacFarlane D.R., Ohno H. & Scrosati B. (2009). Ionic-liquid materials for the electrochemical challenges of the future, *Nature Mater., Vol. 8*, 621-629.
[5] MacFarlane D.R., Tachikawa N., Forsyth M., Pringle J.M., Howlett P.C., Elliott G.D., Davis J.H., Watanabe M., Simon P. & Angell C.A. (2014). Energy applications of ionic liquids, Energy Environ, *Sci., Vol. 7*, 232-250.
[6] Lin M.-C., Gong M., Lu B.G., Wu Y.P., Wang D.-Y., Guan M.Y., Angell M., Chen C.X., Yang J., Hwang B.-J. & Dai H.J. (2015). An ultrafast rechargeable aluminium-ion battery, *Nature, Vol. 520*, 325-328.
[7] Zhong C., Deng Y.D., Hu W.B., Qiao J.L., Zhang L. & Zhang J.J. (2015). A review of electrolyte materials and compositions for electrochemical supercapacitors, *Chemical Society Reviews, Vol. 44*, 7484–7539.
[8] Sippel P., Lunkenheimer P., Krohns S., Thoms E. & Loidl A. (2015). Importance of liquid fragility for energy applications of ionic liquids, *Sci. Rep., Vol. 5*, 13922.
[9] Schuller J., Richert R. & Fischer E. W. (1995). Dielectric relaxation of liquids at the surface of a porous glass, *Phys. Rev. B, Vol. 52*, 15232.
[10] Arndt M., Stannarius R., Groothues H., Hempel E. & Kremer F. (1997). Length Scale of Cooperativity in the Dynamic Glass Transition, *Phys. Rev. Lett., Vol. 79*, 2077.
[11] Barut G., Pissis P., Pelster R. & Nimtz G. (1998). Glass Transition in Liquids: Two versus Three-Dimensional Confinement, *Phys. Rev. Lett., Vol. 80*, 3543.
[12] Pelster R. (1999). Dielectric spectroscopy of confinement effects in polar materials, *Phys. Rev. B, Vol. 59*, 9214.
[13] Alba-Simionesco C., Coasne B., Dosseh G., Dudziak G., Gubbins K. E., Radhakrishnan R. & Sliwinska-Bartkowiak M. (2006). Effects of confinement on freezing and melting, *J. Phys.: Condens. Matter, Vol. 18*, R15.
[14] Fischer J.K.H., Sippel P., Denysenko D., Lunkenheimer P., Volkmer D. & Loidl A. (2015). Metal-organic frameworks as host materials of confined supercooled liquids, *J. Chem. Phys. Vol. 143*, 154505.
[15] Iacob C., Sangoro J. R., Papadopoulos P., Schubert T., Naumov S., Valiullin R., Kärger J. & Kremer F. (2010). Charge transport and diffusion of ionic liquids in nanoporous silica membranes, *Phys. Chem. Chem. Phys., Vol. 12*, 13798–13803.
[16] Iacob C., Sangoro J. R., Kipnusu W. K., Valiullin R., Kärger J. & Kremer F. (2012). Enhanced Charge Transport in Nano-Confined Ionic Liquids, *Soft Matter, Vol. 8*, 289–293.
[17] Perkin S. (2012). Ionic liquids in confined geometries, *Phys. Chem. Chem. Phys., Vol. 14*, 5052–5062.
[18] Li S., Han S. K., Feng G., Hagaman E. W., Vlcek L. & Cummings P. T. (2013). Dynamic and structural properties of room-temperature ionic liquids near silica and carbon surfaces, *Langmuir, Vol. 29*, 9744.
[19] Kondrat S., Wu P., Qiao R. & Kornyshev A. A. (2014). Accelerating charging dynamics in subnanometre pores, *Nature Mater., Vol. 13*, 387–393.
[20] Singh M.P., Verma Y.L., Gupta A.K., Singh R.K. & Chandra S. (2014). Changes in Dynamical Behavior of Ionic Liquid in Silica NanoPores, *Ionics, Vol. 20*, 507–516.
[21] Singh M.P., Singh R.K. & Chandra S. (2014). Ionic Liquids Confined in Porous Matrices: Physicochemical Properties and Applications, *Prog. Mater. Sci., Vol. 64*, 73–120.
[22] Biswas S., Grzywa M., Nayek H. P., Dehnen S., Senkovska I., Kaskel S. & D. Volkmer (2009). A cubic coordination framework constructed from benzobistriazolate ligands and zinc ions having selective gas sorption properties, *Dalton Trans., Vol. 33*, 6487.
[23] Janiak C. (2003). Engineering coordination polymers towards applications, *Dalton Trans., Vol. 14*, 2781.

[24] James S. L. (2003). Metal-organic frameworks, *Chem. Soc. Rev., Vol. 32*, 276.
[25] Kitagawa S., Kitaura R. & Noro S. (2004). Functional Porous Coordination Polymers, *Angew. Chem., Vol. 43*, 2334.
[26] Janiak C. & Vieth J. K. (2010). MOFs, MILs and more: concepts, properties and applications for porous coordination networks (PCNs), *New J. Chem., Vol. 34*, 2366.
[27] Wang C., Liu D. & Lin W. (2013). Metal–Organic Frameworks as A Tunable Platform for Designing Functional Molecular Materials, *J. Am. Chem. Soc., Vol. 135*, 13222.
[28] Furukawa H., Cordova K. E., O'Keeffe M. & Yaghi O. M. (2013). The chemistry and applications of metal-organic frameworks, *Science, Vol. 341*, 1230444.
[29] Usman M., Mendiratta S. & Lu K.-L. (2015). Metal–Organic Frameworks: New Interlayer Dielectric Materials, *ChemElectroChem, Vol. 2*, 786 – 788.
[30] Sippel P., Denysenko D., Loidl A., Lunkenheimer P., Sastre G. & Volkmer D. (2014). Dielectric Relaxation Processes, Electronic Structure, and Band Gap Engineering of MFU-4-type Metal-Organic Frameworks: Towards a Rational Design of Semiconducting Microporous Materials, *Adv. Funct. Mater., Vol. 24*, 3885.
[31] Sippel P., Dietrich V., Reuter D., Aumüller M., Lunkenheimer P., Loidl A. & Krohns S. (2016). Impact of water on the charge transport of a glass-forming ionic liquid, *J. Mol. Liq., Vol. 223*, 635-642.
[32] Lunkenheimer P., Krohns S., Riegg S., Ebbinghaus S. G., Reller A. & Loidl A. (2010). Colossal dielectric constants in transition-metal oxides, *Eur. Phys. J spec. Top., Vol. 180*, 61–89.
[33] Lunkenheimer P., Bobnar V., Pronin A.V., Ritus A.I., Volkov A.A. & Loidl A. (2002). Origin of apparent colossal dielectric constants, *Phys. Rev. B, Vol. 66*, 052105.
[34] Jonscher A. K. (1977). Universal dielectric response, *Nature (London), Vol. 267*, 673-679.
[35] Angell C.A. (1985). Strong and fragile liquids, in: K.L. Ngai and G.B. Wright (Eds.), Relaxations in complex systems, *NRL, Washington DC*, pp. 3-11.
[36] Richert R. (2010). Dielectric spectroscopy and dynamics in confinement, *Eur. Phys. J.: Spec. Top., Vol. 189*, 37.
[37] Ediger M. D., Angell C. A. & Nagel S. R. (1996). Supercooled Liquids and Glasses, *J. Phys. Chem., Vol. 100*, 13200.